

Eukaryotic Initiation Factor (eIF) 1 Carries Two Distinct eIF5-binding Faces Important for Multifactor Assembly and AUG Selection^{*[5]}

Received for publication, October 2, 2007, and in revised form, November 1, 2007. Published, JBC Papers in Press, November 1, 2007, DOI 10.1074/jbc.M708155200

Mikhail Reibarkh^{†1}, Yasufumi Yamamoto^{§1}, Chingakham Ranjit Singh^{§1}, Federico del Rio[‡], Amr Fahmy[‡], Bumjun Lee[§], Rafael E. Luna[‡], Miki Ii[§], Gerhard Wagner^{†2}, and Katsura Asano^{§3}

From the [†]Department of Biological Chemistry and Molecular Pharmacology, Harvard Medical School, Boston, Massachusetts 02115 and the [§]Molecular, Cellular, and Developmental Biology Program, Division of Biology, Kansas State University, Manhattan, Kansas 66506

Eukaryotic initiation factor (eIF) 1 is a small protein (12 kDa) governing fidelity in translation initiation. It is recruited to the 40 S subunit in a multifactor complex with Met-tRNA^{Met}, eIF2, eIF3, and eIF5 and binds near the P-site. eIF1 release in response to start codon recognition is an important signal to produce an 80 S initiation complex. Although the ribosome-binding face of eIF1 was identified, interfaces to other preinitiation complex components and their relevance to eIF1 function have not been determined. Exploiting the solution structure of yeast eIF1, here we locate the binding site for eIF5 in its N-terminal tail and at a basic/hydrophobic surface area termed KH, distinct from the ribosome-binding face. Genetic and biochemical studies indicate that the eIF1 N-terminal tail plays a stimulatory role in cooperative multifactor assembly. A mutation altering the basic part of eIF1-KH is lethal and shows a dominant phenotype indicating relaxed start codon selection. Cheung *et al.* recently demonstrated that the alteration of hydrophobic residues of eIF1 disrupts a critical link to the preinitiation complex that suppresses eIF1 release before start codon selection (Cheung, Y.-N., Maag, D., Mitchell, S. F., Fekete, C. A., Algire, M. A., Takacs, J. E., Shirokikh, N., Pestova, T., Lorsch, J. R., and Hinnebusch, A. (2007) *Genes Dev.* 21, 1217–1230). Interestingly, eIF1-KH includes the altered hydrophobic residues. Thus, eIF5 is an excellent candidate for the direct partner of eIF1-KH that mediates the critical link. The direct interaction at eIF1-KH also places eIF5 near the decoding site of the 40 S subunit.

In eukaryotic translation, initiation factors (eIFs)⁴ promote dissociation of the 80 S ribosome. They assist binding of Met-

tRNA^{Met} and 5'-capped mRNA to the 40 S subunit to form 43 S and 48 S preinitiation complexes, respectively (for a review, see Refs. 1 and 2). The 43 S complex contains eIF1A, eIF1, eIF5, eIF3, and the eIF2·GTP·Met-tRNA^{Met} ternary complex (TC). The eIF4E subunit of eIF4F binds the 5' cap of mRNA, whereas its eIF4G subunit binds eIF3 in mammals and eIF5 in yeast to recruit the latter factors to the mRNA. The RNA helicase eIF4A and its cofactor eIF4B are required for unwinding the 5'-terminal region of the capped mRNA. The resulting preinitiation complex termed 48 S is believed to undergo the scanning process to position the preinitiation complex onto the first AUG codon of the mRNA.

Prior to AUG recognition, GTP bound to eIF2 appears to be hydrolyzed by the action of the N-terminal residues of eIF5 through a mechanism stimulated by 48 S complex formation. Upon Met-tRNA^{Met} anticodon pairing with the start codon, the P_i resulting from the GTP hydrolysis is released (3). These events, coupled with a ribosomal conformational change (4, 5), trigger dissociation of eIF1 and eIF2·GDP. The GTPase switch eIF5B promotes joining of the resulting 40 S initiation complex with the 60 S subunit to produce the 80 S initiation complex, an immediate precursor for protein synthesis elongation. The GDP-bound eIF2 is recycled to eIF2·GTP by the action of the pentameric guanine nucleotide exchange factor eIF2B.

eIF1, encoded by *SUI1* in yeast *Saccharomyces cerevisiae*, plays a central role in ensuring the fidelity of translation initiation by destabilizing ribosomal complexes assembled on non-cognate and poorly contexted start codons (6) and by repressing the GTPase activating activity of eIF5 or release of P_i until precise AUG pairing to the tRNA^{Met} anticodon (3, 7). Yeast eIF1 binds concurrently to eIF5-CTD as well as to the eIF2β and eIF3c subunits, thereby being recruited to the 40 S subunit in the multifactor complex (MFC) formed with eIF2 TC, eIF3, and eIF5 (8, 9). Except for the small eIF1 (12 kDa), minimal binding domains of yeast MFC constituents were identified to be eIF2β-(1–140), eIF3c-(1–156), and eIF5-(241–405) (8, 10). Of these, eIF2β-(1–140) and eIF3c-(1–156) are charged hydrophilic polypeptides. eIF2β-(1–140) regulates the affinity of eIF5-CTD-(241–405) for eIF3c-(1–156), thereby promoting MFC

^{*} This work was supported by National Institutes of Health Grants GM64781 (to K. A.) and CA68262 and GM47467 (to G. W.). The costs of publication of this article were defrayed in part by the payment of page charges. This article must therefore be hereby marked "advertisement" in accordance with 18 U.S.C. Section 1734 solely to indicate this fact.

[5] The on-line version of this article (available at <http://www.jbc.org>) contains supplemental Table S1.

The atomic coordinates and structure factors (code 2OGH) have been deposited in the Protein Data Bank, Research Collaboratory for Structural Bioinformatics, Rutgers University, New Brunswick, NJ (<http://www.rcsb.org>).

¹ These authors contributed equally to this work.

² To whom correspondence may be addressed. E-mail: gerhard_wagner@hms.harvard.edu.

³ To whom correspondence may be addressed. E-mail: kasano@ksu.edu.

⁴ The abbreviations used are: eIF, eukaryotic initiation factor; TC, ternary complex; MFC, multifactor complex; NTT, N-terminal tail; CTD, C-terminal

domain; ORF, open reading frame; uORF, upstream ORF; FOA, 5-fluoroorotic acid; sc, single copy; hc, high copy; GST, glutathione S-transferase; aa, amino acids.

TABLE 1
Plasmids and yeast strains with different eIF1 mutations

Allele	eIF1 amino acid change(s)	T7 cloning plasmid	GST fusion plasmid	sc <i>SUI1 LEU2</i> CEN plasmid	<i>gcn2Δ</i> strains ^a
Wild type <i>SUI1</i> ⁺	Wild type	pT7-SUI1 ^b	pGEX-SUI1 ^a	YCpL-SUI1 ^c	KAY230
NTT mutations					
<i>M1</i>	aa. 5–12 to DYKDDDDK	pET-SUI1-M1	NC ^d	YCpL-SUI1-M1	KAY333, KAY525
<i>M2</i>	aa. 11–18 to DYKDDDDK	pET-SUI1-M2	NC	YCpL-SUI1-M2	KAY286
<i>M3</i>	Leu ⁶ , Phe ⁹ , and Phe ¹² to Gln	pET-SUI1-M3	NC	YCpL-SUI1-M3	KAY539
<i>Δ20</i>	Deletion of aa. 2–21	NC	NC	YCpL-SUI1Δ20	KAY541
<i>FL-SUI1</i> ^e	DYKDDDDKL after aa 1	pET-FL-SUI1 ^{c,f}	NC	YCpL-FL-SUI1 ^{ac}	KAY528
Basic surface mutations					
<i>M4</i>	Lys ¹⁰⁰ , Lys ¹⁰¹ , Lys ¹⁰⁴ , and His ¹⁰⁶ to Gln	pT7-SUI1-M4	NC	YCpL-SUI1-M4	NA ^e
<i>M5</i>	Lys ⁵² , Arg ⁵³ , Lys ⁵⁶ , Lys ⁵⁹ , and Lys ⁶⁰ to Ala	pET-SUI1-M5	pGEX-SUI1-M5	YCpL-SUI1-M5	NA
Other constructs					
<i>sui1-1</i>	Asp ⁸³ to Gly	pT7-SUI1-1 ^b	NC	NC	NC
<i>His-SUI1</i>	Six His after aa 1	pET-His-SUI1	NC	YCpL-His-SUI1	KAY250
<i>SUI1-His</i>	Six His after aa 108	pET-SUI1-His	NC	YCpL-SUI1-His	NA

^a Isogenic to KAY230 (MAT α *leu2 lys11 ura3-52 trp1Δ mof2(sui1)::hisG gcn2::hisG* p[*SUI1 LEU2*]) except carrying a *sui1 LEU2* CEN plasmid listed in column 4 instead of p[*SUI1 LEU2*].

^b Constructed in Ref. 19.

^c Constructed in Ref. 9.

^d NC, not constructed for this study.

^e NA, not applicable because the allele used is unconditionally lethal.

^f pET-FL-SUI1 has DYKDDDDKM after aa. 1, instead of DYKDDDDKL.

assembly (11). The interaction of eIF3c-(1–156) with eIF1 is important for rapid 43 S-48 S complex formation, and initiation fidelity is governed by eIF1 (7). The C-terminal minimal MFC binding domain, eIF5-CTD-(241–405), forms a HEAT domain fold with eight α -helices (12, 13). It binds to eIF1 and eIF3c and to eIF2 β at two conserved basic and acidic surface sites termed area II and area I, respectively (14). The eIF5 C-terminal tail (aa 396–405) also contributes to eIF2 β binding (14).

Human eIF1 exhibits a globular α/β core and an unstructured N-terminal tail (NTT) (15). Hydroxyl-radical footprinting studies identified a surface of its globular core as facing the rRNA helix 24 close to but separated from the P-site (16). N-terminal FLAG tagging of yeast eIF1 impairs its interaction with eIF2 β and eIF5 and reduces TC binding to the ribosome *in vivo*, suggesting that the eIF1-NTT is important for MFC formation. Chueng *et al.* (17) recently confirmed this idea by finding that the alteration of Phe⁹ and Phe¹² residues of eIF1-NTT to alanines impairs partial 43 S complex assembly *in vitro*. However, the direct physical evidence that eIF1-NTT binds eIF5 or eIF2 β has been lacking. Here we report the solution structure of yeast eIF1 and its binding sites for eIF5-(241–405) as determined with NMR spectroscopy. These studies identify NTT and a basic/hydrophobic surface of the globular core termed KH as binding sites for eIF5-CTD. Remarkably, the above mentioned report by Chueng *et al.* (17) further showed that the hydrophobic residues, found here in the eIF1-KH area, also mediate a critical link to the preinitiation complex that suppresses eIF1 release before start codon selection. We propose that eIF5 is an excellent candidate for the direct partner of eIF1-KH that produces such a link.

MATERIALS AND METHODS

Plasmids and Yeast Strains—Plasmids and yeast strains encoding wild-type, His₆-tagged, or mutant forms of eIF1 were constructed as follows and listed in Table 1. All of the oligonucleotides used in this study are listed in Table S1.

To create pET-His-SUI1, the 0.7-kb NdeI-HindIII fragment of the PCR product, using oligonucleotides eIF1-Nde and eIF1-Hd (Table 1) and p1128 (18) as template, was cloned into pET15b (Novagen). Then the 0.2-kb NcoI-BamHI fragment of pET-His-eIF1 (the NcoI site is located in pET15b upstream of the *His-SUI1* ORF) was cloned into YCpL-SUI1ΔNco (9) to create YCpL-His-SUI1. To prepare pET-SUI1-His, the 0.33-kb NdeI-SalI SUI1-His ORF fragment from PCR with oligonucleotides eIF1-Nde and eIF1-His-RV and the 0.31-kb SalI-HindIII 3'-UTR fragment from PCR with oligonucleotides eIF1-Sal and eIF1-Hd were cloned together into pET23a (Novagen). Then the 0.7-kb NdeI-HindIII fragment of pET-SUI1-His was cloned into YCpL-SUI1ΔNde (9) to obtain YCpL-SUI1-His.

All of the mutants except *M4* were created by subcloning the 0.21-kb NdeI-BamHI DNA fragment corresponding to the 5'-half of the mutant eIF1 ORF, generated by PCR as follows, into YCpL-SUI1ΔNde (9). To prepare the *SUI1-M1*, *-M2*, *-M3*, or *-Δ20* segments, PCR was performed with the corresponding mutating primer, the oligonucleotide UFW, and YCpL-SUI1 DNA as template, creating a 0.7-kb DNA fragment with the mutant eIF1 ORF and 3'-untranslated region, followed by NdeI and BamHI digestion. To create the *SUI1-M5* mutant segment, oligonucleotides eIF1-Nde and eIF1-M5-RV were used for PCR.

To create YCpL-SUI1-M4, we first produced two DNA fragments from separate PCR, one using oligonucleotides eIF1-Nde and eIF1-M4-RV and the other using eIF1-M4-FW and UFW. In both reactions, YCpL-SUI1 was used as a template. Following DpnI digestion (to remove contamination of bacterially produced and hence methylated YCpL-SUI1), these two segments (0.3 and 0.4 kb in size, respectively) were gel-purified and combined to perform the second PCR using primers eIF1-Nde and UFW. The 0.4-kb NdeI-HindIII fragment of YCpL-SUI1ΔNde was replaced with that of the 0.7-kb product of the second PCR.

To create pET- and pGEX-derivatives of the site-directed mutants, listed in Table 1, the 0.7-kb NdeI-HindIII fragments of YCpL-SUI1 derivatives were cloned into the same sites of

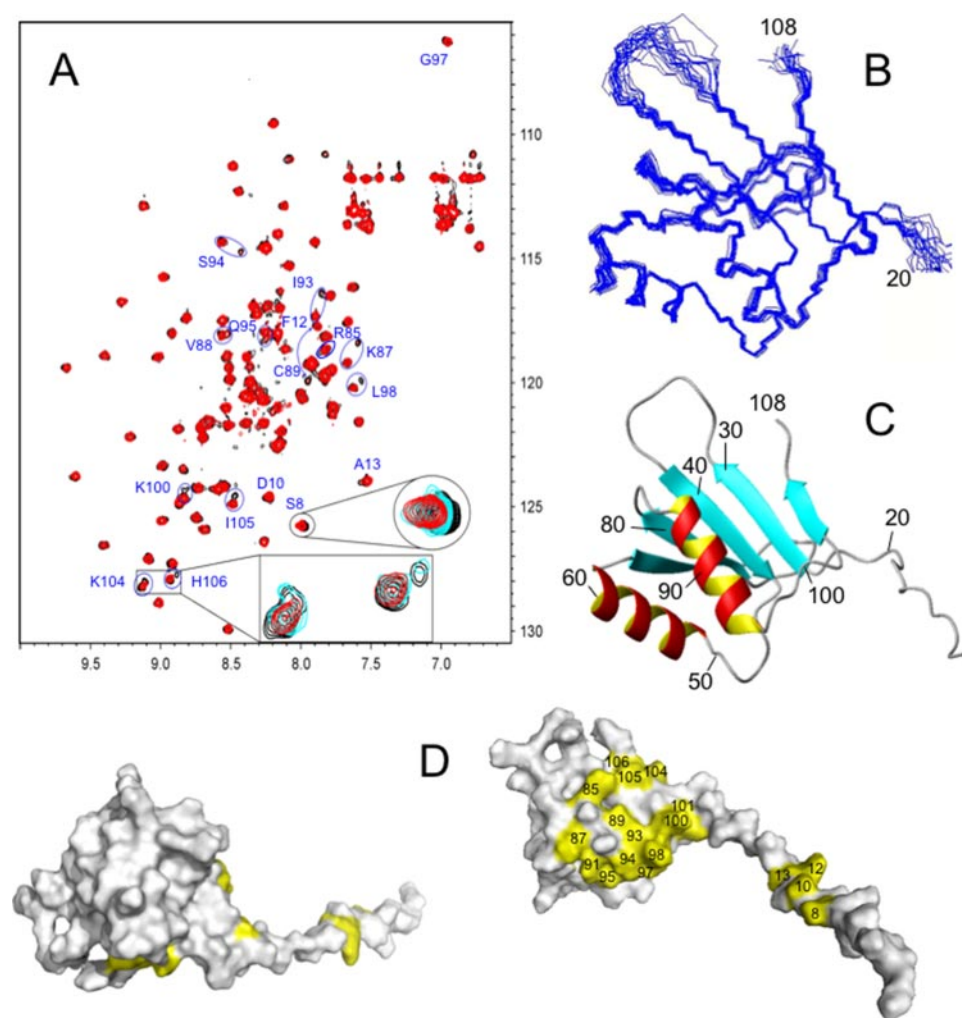


FIGURE 1. Solution structure of yeast eIF1 and identification of the eIF5-binding site using chemical shift mapping. A, superposition of ^1H - ^{15}N HSQC spectra of $75\ \mu\text{M}$ eIF1-His alone (black) and in the presence of $750\ \mu\text{M}$ GB1-eIF5-(241–405) (red). Residues affected are identified with blue labels. Cross-peaks from the NTT show simple chemical shift changes dependent on the concentration of GB1-eIF5-(241–405). An expansion of the cross-peak for S8 shows this effect for three ligand concentrations (0-, 5-, and 10-fold excess in black, blue, and red). Ellipses and arrows identify residues with two conformations, for which the minor conformation disappears upon the addition of GB1-eIF5-(241–405). As an example, the expansion of the signals for Lys¹⁰⁴ and His¹⁰⁶ shows that the intensity of the signals of the minor form decreases in dependence on the GB1-eIF5-(241–405) concentration. Nearly identical results were obtained in titration experiments with $0.2\ \text{M}$ eIF1. All spectra were recorded at $1\ \text{M}$ NaCl, pH 7.2. B, ensemble of yeast eIF1 models (residues 20–108) calculated from the NMR data. C, ribbon diagram of the globular core of yeast eIF1. D, surface representation of eIF1. The residues of eIF1 affected by the addition of eIF5-CTD are colored in yellow. Right, same orientation as in B and C; left, orientation turned by 180° around the x axis. All affected residues are located on one face of the globular domain and in the NTT.

pET23a (Novagen) and pGEX-TIF35 (19), respectively. pGEX-SUI1* was constructed by subcloning the 0.8-kb NdeI-HindIII fragment of pT7-SUI1 into pGEX-TIF35. pGEX-SUI1* is different from pGEX-SUI1 (20) in that the latter has an insertion of a FLAG epitope between the GST and eIF1 moieties. Although we created pGEX-SUI1* to remove concerns from the effect of the FLAG peptide, we did not observe any difference between the results of binding experiments performed with these constructs. Valasek *et al.* used pGEX-SUI1* as a control to test the effect of *sui1-1* on eIF3c binding (7). pT7-SUI1-M4 was constructed by subcloning the 0.42-kb AflII-HindIII fragment of YCpL-SUI1-M4 into the same sites of pT7-SUI1 (19).

Besides the plasmids listed in Table 1, the following plasmids were constructed in this study. YEPL-SUI1-M4 and -M5 were

prepared by transferring the SacI-HindIII 1.2-kb *SUI1* fragment of the corresponding single copy (sc) mutant plasmid derivatives (Table 1) to YEplac181 (21). YCpU-SUI1-M4 and -M5 were likewise constructed by transferring the same segment of sc mutant derivatives to YCplac33 (21). To better express unmodified eIF1 in bacteria, we created pET-SUI1 by subcloning the 0.7-kb NdeI-HindIII wild-type *SUI1* fragment from PCR with oligonucleotides eIF1-Nde and eIF1-Hd into pET23a. pET-SUI1-1-His, encoding the *sui1-1* (D83G) mutant form of eIF1-His, was constructed by subcloning into pET23a the 0.35-kb NdeI-SalI *SUI1-1-His* ORF segment from PCR using oligonucleotides eIF1-Nde and eIF1-His-RV and a *sui1-1* plasmid as template. The 0.7-kb NdeI-HindIII fragments of YCpL-SUI1-M1 to -M5 were subcloned into pET23a to create pET-His-SUI1-M1 to -M5. The products of these plasmids were used to analyze the folding of the corresponding mutant forms of eIF1 (Fig. 3).

pGB-TIF5-B6 was constructed by subcloning the PCR-amplified BamHI fragment of eIF5 (aa 241–405) ORF into pGBfusion1 (22). pGB1-TIF5-B5.5-BN1 encoding the GB1 fusion form of BN1 mutant eIF5-(220–405) will be described elsewhere.⁵

The *GCN2* allele in KAY146 (Table 1) was deleted using pHQ414 (*gcn2::hisG::URA3::hisG*) as described (23) to generate KAY230 (Table 1).

The *LEU2 SUI1* plasmid in this strain was replaced with the *URA3 SUI1* plasmid by naturally segregating the former from a KAY230 transformant carrying the latter to select KAY231. KAY231 was then used for plasmid shuffling using the drug 5-fluoroorotic acid (FOA) (24) to create all of the *SUI1* mutant strains listed in column 6 of Table 1. Briefly, the Ura3p enzyme converts FOA into a toxic compound. Thus, the growth of a KAY231 transformant carrying a YCpL-SUI1 (*LEU2*) derivative (Table 1, column 5) on the FOA medium selects for a *sui1Δ* strain lacking p(*URA3 SUI1*) but still containing the mutant YCpL-SUI1 derivative (Table 1, column 6) if the mutant *SUI1* allele is not lethal.

NMR Spectroscopy—Sample preparation and spectra measurement for NMR spectroscopy were done as described in Ref.

⁵ B. Lee and K. Asano, manuscript in preparation.

25. NMR experiments for eIF1 backbone assignment and structure determination have been carried out with the sample of 0.9 mM ^{15}N -, ^{13}C -labeled eIF1 in a buffer containing 20 mM Tris, 300 mM NaCl, 5 mM β -mercaptoethanol, pH 7.2. Binding NMR experiments have been carried out in 20 mM Tris, 1 M NaCl, 5 mM β -mercaptoethanol, pH 7.2, buffer with 0.075 mM ^{15}N eIF1 and 0.075–1.5 mM unlabeled GB1-eIF5-(241–405). Structural figures were produced with MolMol and PyMOL (available on the World Wide Web). To investigate whether the eIF1 mutants described here are folded, we expressed ^{15}N -labeled M1–M5 mutant forms of His-eIF1 and the D83G form of eIF1-His and recorded ^1H - ^{15}N correlated HSQC spectra.

Biochemical Techniques—Protein interactions *in vitro* (11) and the preinitiation complex formation *in vivo* (26, 27) were assayed as described previously.

RESULTS

Solution Structure of Yeast eIF1 and Identification of the eIF5-binding Face—To study the effect of eIF5-(241–405) on the structure of yeast eIF1, we first studied NMR spectra of its C-terminally or N-terminally hexahistidine-tagged forms termed eIF1-His and His-eIF1 alone. *In vivo* assessment of the function of eIF1-His and His-eIF1 is described in the supplemental materials. Both eIF1 constructs exhibited excellent two-dimensional ^1H - ^{15}N HSQC spectra, indicating that the protein is well behaved and folded with His₆ tags on either termini. Fig. 1A displays the ^1H - ^{15}N HSQC spectrum of eIF1-His in *black*. The resonances were assigned, using standard multiple-resonance experiments, and the structure was determined as described previously for human eIF1 (15), except that CYANA was used for structure calculation instead of XPLOR. The resulting structure of the globular core (residues 24–108) is shown in Fig. 1, B and C (Table 2). As expected from the high sequence homology (87% similarity and 63% identity), the structure is very similar to that of human eIF1 (15). However, in contrast to the human protein, yeast eIF1 contains a segment (residues 87–106) that adopts two distinct but similar conformations as manifested with two sets of backbone resonances for 13 of the 20 residues, and the resonances of both forms could be assigned unambiguously (Fig. 1A). The two conformations are in slow exchange, since two sets of signals are observed. The relative populations are salt-dependent, and the minor conformation at high salt becomes the major conformation at low salt. The dependence of relative signal intensities on the salt concentration identifies this effect as two interconverting conformations rather than a heterogeneity of the covalent structure. The small differences of chemical shifts show that the two structures must be very similar and would be difficult to individually determine with NMR spectroscopy.

To identify the binding site for eIF5, we pursued an NMR mapping approach. Since previous evidence suggested that the eIF1-binding activity of eIF5 resides in its C-terminal domain (9), we expressed C-terminal fragments with different sizes. Among these, an eIF5-(241–405) fragment behaved best in terms of solubility and NMR spectral appearance. However, even this segment aggregated and exhibited poor NMR spectra. Thus, we used a N-terminal fusion with the B1 domain of streptococcal protein G (GB1) as a solubility enhancement tag (22).

TABLE 2

Statistical parameters for an ensemble of 20 calculated eIF1 solution structures

Parameters	Values
CYANA target function (\AA^2)	0.8 ± 0.1
No. of “acting” distance constraints (upper/lower)	
Nuclear Overhauser effect	570/0
Hydrogen bond	72/72
No. of torsion constraints	
Backbone	174
χ angles	39
Upper constraint violations	
Root mean square	0.02 ± 0.002
Maximum (\AA)	0.18
Lower constraint violations	
Root mean square	0.01 ± 0.002
Maximum (\AA)	0.02, 0.06
Angle constraint violations	
Root mean square	0.25 ± 0.05
Maximum (degrees)	2.6
van der Waals distance violations	
Sum	2.4 ± 0.3
Maximum (\AA)	0.27
Root mean square deviations to mean structure (\AA)	
Full protein without NTT (residues 24–108)	0.6 ± 0.2
Backbone	
All heavy atoms	1.3 ± 0.3
Protein without all flexible regions (residues 24–30, 39–69, 77–108)	0.4 ± 0.1
Backbone	
All heavy atoms	1.0 ± 0.2

This fusion protein behaved well and exhibited good NMR spectra but required high salt concentrations to remain monomeric. At high salt, the eIF1/eIF5 interaction is rather weak but clearly identifiable in the NMR experiments (see below). Lower salt increases the affinity but causes broadening of both the eIF1 and eIF5 spectra so that spectral changes cannot be monitored.

Thus, all NMR titrations had to be carried out at 1 M NaCl. We added unlabeled GB1-eIF5-(241–405)-His to the two differently tagged forms of eIF1. Only eIF1-His was affected by the addition of GB1-eIF5-(241–405)-His, consistent with *in vitro* binding studies showing that an N-terminal His tag prevents binding, as mentioned above. Of 108 yeast eIF1 amino acids, 17 were affected by eIF5-(241–405) (Fig. 1A). Among these, residues Ser⁸, Asp¹⁰, Phe¹², and Ala¹³ are located in the unstructured NTT and experience ligand-dependent chemical shift changes (fast exchange limit). The second group consists of Arg⁸⁵, Lys⁸⁷, Val⁸⁸, Cys⁸⁹, Phe⁹¹, Ile⁹³, Ser⁹⁴, Gln⁹⁵, Gly⁹⁷, Leu⁹⁸, Lys¹⁰⁰, Lys¹⁰¹, Lys¹⁰⁴, Ile¹⁰⁵, and His¹⁰⁶. These residues adopted two conformations in free eIF1 (see above); the addition of GB1-eIF5-(241–405)-His caused the minor conformation to disappear in a manner proportional to the ligand concentration. This indicates that eIF5 binding competes with the intramolecular interactions that stabilize the minor conformation. All affected residues cluster in two separate regions of eIF1 (Fig. 1D) defining potential binding sites for eIF5-(241–405), one at the NTT (aa 1–23) and the other at a basic surface area of the globular core (Fig. 1D). We call this site the KH area after the characteristic lysine (**K**) and hydrophobic residues.

To confirm that the basic surface of eIF5-(241–405) is the primary eIF1-binding face (14), we mixed ^{15}N -labeled eIF1-His with the B1 mutant form of GB1-eIF5-(220–405)-His, altering six basic amino acids (Lys³⁶⁷, Lys³⁶⁰, Lys³⁷², Lys³⁷⁵, Lys³⁷⁹,

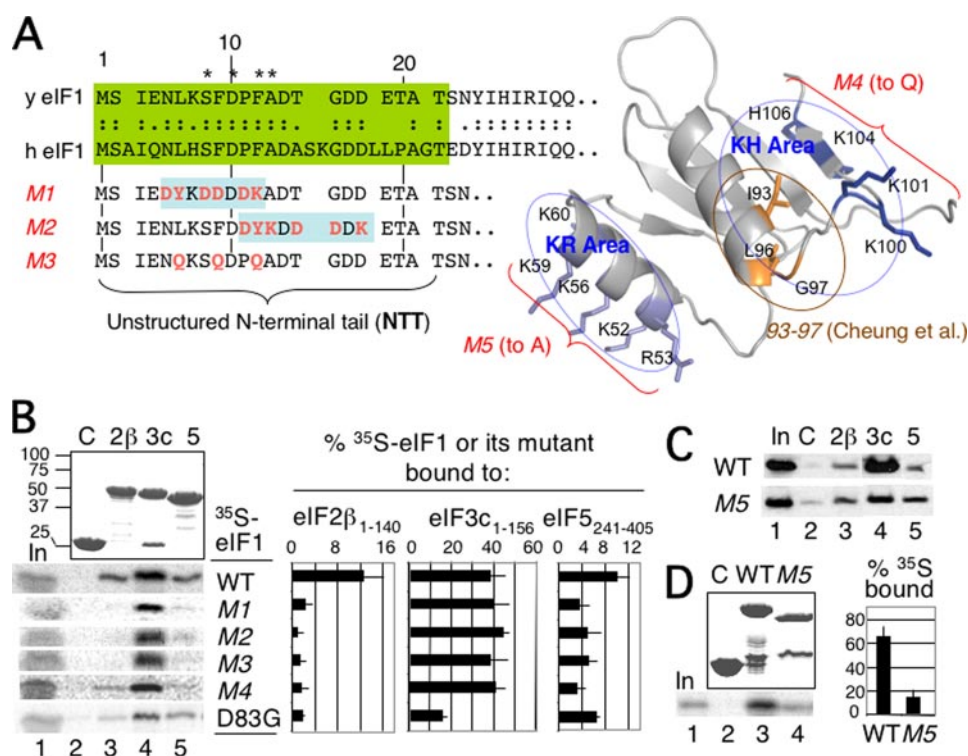


FIGURE 2. Effect of eIF1 mutations on eIF partner interactions *in vitro*. *A*, the amino acid sequence of yeast eIF1 (*y eIF1*) in its NTT is highlighted in green, together with aligned human eIF1 sequence. The amino acid sequences of the site-directed mutants are indicated below with their clone names indicated to the left. The asterisks on top show the NTT amino acids affected by eIF5 in NMR studies (Fig. 1). Shown in red are altered amino acids. Boxed with light blue are the FLAG epitope sequences introduced. Right, ribbon model of yeast eIF1 (this study), indicating the positions of M4, M5 (this study), and 93–97 (17) as well as the location of KH and KR areas. *B*, 5 μg of GST alone (*C*, lane 2), GST-eIF2β-(1–140) (9) (2β, lane 3), GST-eIF3c-(1–156) (8) (3c, lane 4), and GST-eIF5-(241–405) (10) (5, lane 5) was allowed to bind ³⁵S-labeled eIF1 or its derivative that had been expressed in the TNT System (Promega) from appropriate plasmids (Table 1, column 3). The complex was isolated and analyzed by SDS-PAGE followed by Coomassie staining (top gels) and a STORM PhosphorImager (Amersham Biosciences) (second to bottom gels), as described (11). Lanes 1, 10% input amounts. Average percentage of ³⁵S-protein bound (boxes) and S.D. values (lines) from these and more than two more independent experiments are summarized to the right. *C*, GST fusion proteins used in *B* were allowed to bind ~10 μg of recombinant eIF1 or eIF1-M5, expressed in BL21(DE3) carrying pET-SUI1 or pET-SUI1-M5 (Table 1, column 3), respectively, as described (9). Bound eIF1 was analyzed by immunoblotting with anti-eIF1 antibodies. Lane 1, 2% input amount. Note that a minor fraction of eIF1-M5 binds to GST alone in lane 2, suggesting that a part of expressed eIF1-M5 was denatured. This may explain why a slightly higher fraction of eIF1-M5 binds to GST-eIF5 or -eIF2β. *D*, 5 μg of GST alone (lane 2), GST-eIF1 (lane 3), and GST-eIF1-M5 (lane 4), expressed from plasmids in Table 1, column 4, was allowed to bind ³⁵S-labeled His-eIF3c-(1–156) (8), and the complexes were analyzed as in *B*.

and Arg³⁸²) to Gln (see Fig. 7*a* for the basic area II) involved in eIF1 binding. As expected, the *BN1* mutant form of the GB1-eIF5 segment did not change the HSQC spectra of ¹⁵N-labeled eIF1-His (data not shown). The NMR spectrum of GB1-eIF5-(220–405)-His^{BN1} sample displayed well dispersed chemical shifts, confirming that the *BN1* mutant eIF5-CTD is folded (data not shown). Thus, the *BN1* mutation impaired the eIF1/eIF5-(220–405) interaction by altering the surface residues of eIF5 without largely unfolding the structure.

Effect of eIF1-NTT Mutations on Binding to eIF Partners *In Vitro*—Next, we performed site-directed mutagenesis to test the significance of the eIF1-NTT for binding GST fusion forms of MFC partner fragments, eIF5-(241–405), eIF2β-(1–140), and eIF3c-(1–156). As shown in Fig. 2*A*, the *M1* and *M2* mutations change residues 5–12 and 11–18 to the FLAG epitope (DYKDDDDDK). We expressed ³⁵S-labeled wild-type and mutant eIF1 in reticulocyte lysate and tested their interactions. As shown in Fig. 2*B*, both *M1* and *M2* significantly reduced

³⁵S-labeled eIF1 binding to GST-eIF5-(241–405) as well as to GST-eIF2β-(1–140). However, they did not alter its binding to GST-eIF3c-(1–156). Thus, the NTT is an important binding element for eIF5 and eIF2β. Given that the FLAG epitope sequence is rich in acidic residues, we reasoned that hydrophobic residues in the N-terminal half of the eIF1-NTT are important. To test this, we created *SUI1-M3*, altering conserved Leu⁶, Phe⁹, and Phe¹² to polar glutamine residues (Fig. 2*A*). As expected, *M3* impaired eIF1 binding to eIF2β and eIF5 but not to eIF3c (Fig. 2*B*).

Effect of eIF1 Basic Surface Mutations on Binding to eIF Partners *In Vitro*—To examine the basic eIF5-binding face of eIF1, we simultaneously altered Lys¹⁰⁰, Lys¹⁰¹, Lys¹⁰⁴, and His¹⁰⁶ to glutamines, creating mutant *M4*. *M4* also reduced binding to eIF2β and eIF5 but not to eIF3c (Fig. 2*B*). Thus, the interactions of eIF1 with eIF2β and eIF5 depended on the same NTT and basic areas when eIF2β and eIF5 each was the sole binding partner.

Because eIF3c-(1–156) can stabilize the eIF1-eIF5-(241–405) complex by mutual cooperativity (8), we searched for a potential eIF3c-binding face on the surface separate from the eIF5 binding areas. We created mutant *M5* altering Lys⁵², Arg⁵³, Lys⁵⁶, Lys⁵⁹, and Lys⁶⁰ to alanines (Fig. 2*A*), because (i) these

constitute the major conserved basic surface noted earlier (15) and (ii) the eIF1-binding site in eIF3c-(1–156) is highly acidic (7). This conserved basic surface overlaps with the 40 S subunit rRNA-binding site (16). As expected, *M5* reduced both GST-eIF3c-(1–156) binding to bacterially expressed recombinant eIF1 (Fig. 2*C*) and GST-eIF1 binding to ³⁵S-labeled eIF3c-(1–156) (Fig. 2*D*) without affecting interaction with eIF2β and eIF5 (Fig. 2*C*). Thus, we identified the eIF3c-binding face, which is now designated KR for characteristic lysine and arginine residues (Fig. 2*A*). (We used bacterially expressed eIF1-M5 because this construct did not express in the T7 polymerase-coupled reticulocyte system).

We also studied the effect of the spontaneously isolated D83G (*sui1-1*) mutation (18). D83G reduced all of the interactions with eIF2β, eIF3c, and eIF5 (Fig. 2*B*), confirming its previously reported effect on eIF3c binding (7). Given rather a non-specific effect on factor binding, we wondered whether D83G affects the whole structure of the protein. Consistent with this,

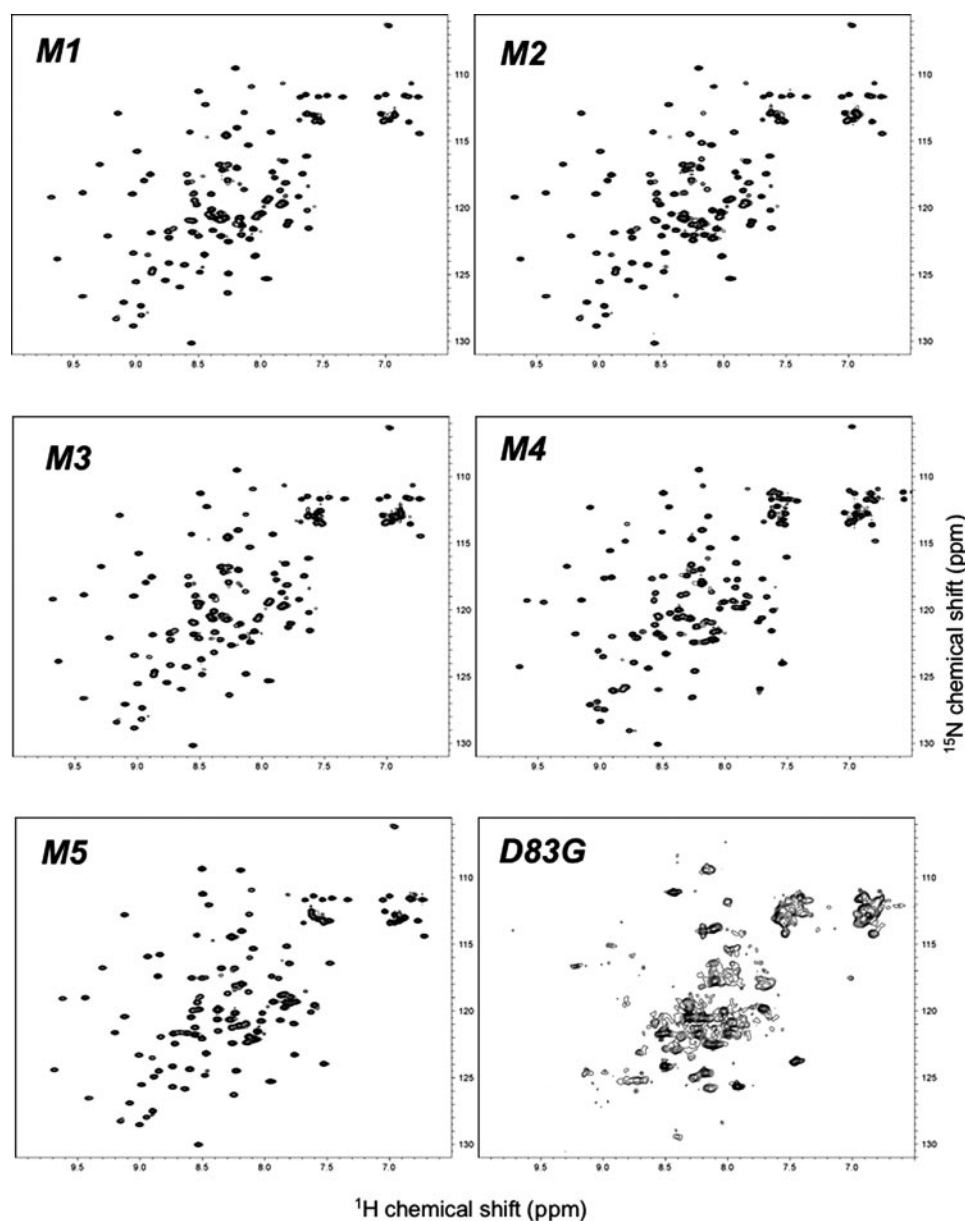


FIGURE 3. ^1H - ^{15}N HSQC spectra of eIF1 mutants. Mutants M1–M5 show spectra nearly identical to that of wild-type eIF1 (Fig. 1A), indicating that the globular fold is conserved. The D83G mutant exhibits an entirely different spectrum with only a few resolved cross-peaks and many broad features. This is evidence that this mutant is at least partially unfolded.

the ^1H - ^{15}N HSQC spectra of ^{15}N -labeled sample of the mutant show significant resonance line broadening and peak disappearance, suggesting at least partial unfolding of the protein (Fig. 3). By contrast, ^{15}N -labeled eIF1 mutants M1–M5 showed ^1H - ^{15}N HSQC spectra of the same quality as wild type, indicating that these new mutants are folded (Fig. 3).

The eIF1-NTT Is Required for Its Cooperative Incorporation into MFC—Having observed that the binary interactions of eIF1 with eIF2 β and eIF5 depend on the same interfaces, NTT and 4KH, we wished to determine which surface is more critical for eIF1 incorporation into the MFC. Thus, we tested the effect of eIF1 mutations on its binding to a binary complex of eIF5-(241–405) and GST-eIF2 β -(1–140), a reaction mimicking cooperative MFC formation (9). We also used, as eIF1 mutants, previously characterized constructs, FL-eIF1 and eIF1-FL, with the

FLAG epitope introduced to the N and C terminus of eIF1, respectively (9); FL-eIF1 becomes important in subsequent *in vivo* studies (see Figs. 5 and 6). In this experiment, ^{35}S -labeled eIF1 was mixed with His-eIF5-(241–405) and GST-eIF2 β -(1–140) in a trace amount compared with the latter two. Subsequently, the complex was pulled down with glutathione resin and analyzed by SDS-PAGE. The data in Fig. 4A, panel 1, and its quantification in Fig. 4B confirmed that eIF1 binding to GST-eIF2 β -(1–140) was >3-fold increased due to bridging by eIF5-(241–405), indicating mutual cooperativity between eIF1 interactions with eIF5 and eIF2 β (9). Likewise, the binding of eIF1-FL greatly increased by the presence of eIF5-(241–405), and the binding of eIF1-M4 was also slightly but significantly increased (Fig. 4, A, panels 4 and 5, and B, columns 3–6). Note that both the mutants would interfere with interaction at the KH interface (also see “Discussion”). In contrast, the NTT mutants M1 and M2 and N-terminal FLAG-eIF1 (FL-eIF1) did not bind at all to the GST-eIF2 β -(1–140)-eIF5-(241–405) complex (Fig. 4A, panels 2, 3, and 6). These results indicate a more critical role for eIF1-NTT in MFC incorporation or formation.

To test if eIF1-NTT mediates eIF1 incorporation into MFC *in vivo*, we expressed mutant eIF1 in yeast encoding HA-eIF3i. As shown in Fig. 4C, HA-tagged eIF3 immunoprecipitates endogenous eIF1

(lanes 5, 8, and 11), but not eIF1-M1 (lane 8) or eIF1-M2 (lane 11), which migrated more slowly than wild-type eIF1 due to amino acid composition changes (*upper bands in third gel*). We previously showed that FLAG-eIF1 is likewise defective in binding to HA-eIF3 in this assay (9). Because the mutant versions of eIF1 under the study were expressed in the presence of wild-type eIF1, the effect of these mutations on eIF1 binding to eIF3 *in vivo* might be minor if it was examined in the absence of wild-type eIF1. Nevertheless, the co-immunoprecipitation studies indicate that the eIF1-NTT plays at least a stimulatory role in its incorporation into the MFC *in vivo*.

The Effect of eIF1 Surface Mutations on Yeast Growth—To study the effect of eIF1 mutations on yeast growth, we introduced sc YCpL-SUI1 plasmid derivatives encoding eIF1 mutants under the natural promoter (Table 1, column 5) to

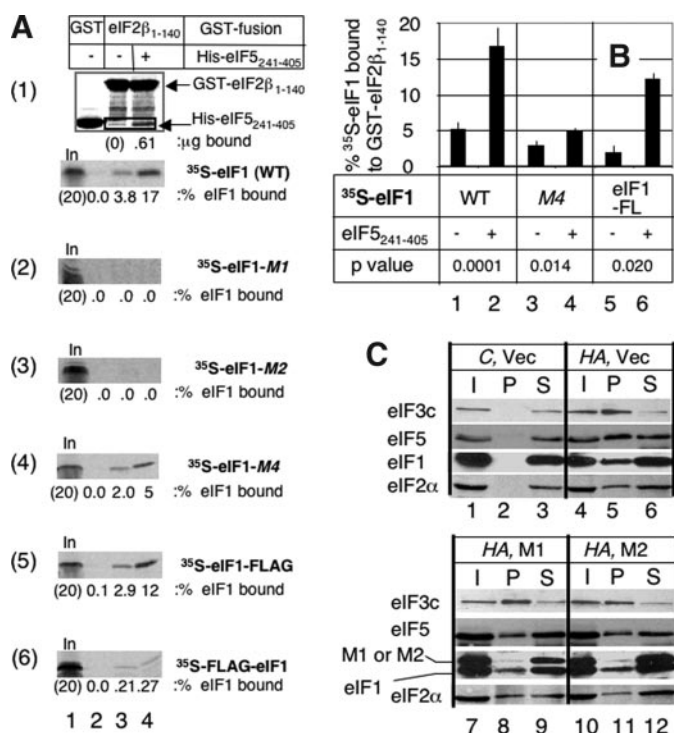


FIGURE 4. Effect of eIF1 mutations on its cooperative binding to eIF5-eIF2β complex. A, GST-eIF2β₁₋₁₄₀ (~5 μg) was incubated with 10 μg of His-eIF5₂₄₁₋₄₀₅ and with ³⁵S-labeled eIF1 or its derivatives (indicated to the right in boldface type) in 200 μl of the binding buffer. The complex containing GST-eIF2β₁₋₁₄₀ was pulled down with glutathione resin, washed twice, and analyzed by SDS-PAGE, as in Fig. 2B. Amounts of ³⁵S-proteins bound to the resin were determined by phosphorimaging analyses of Coomassie-stained SDS-polyacrylamide gels and are shown below each gel. Lanes 1, 20% input amount. In panel 1, the top gel indicates His-eIF5₂₄₁₋₄₀₅ co-precipitated with GST-eIF2β₁₋₁₄₀. His-eIF5₂₄₁₋₄₀₅ was bound similarly in all other panels. B, fractions of ³⁵S-labeled eIF1 (WT), its M4 mutant (eIF1-M4), or C-terminally FLAG-tagged eIF1 (eIF1-FL) bound to the GST-eIF2β₁₋₁₄₀ in the presence (+) or absence (-) of His-eIF5₂₄₁₋₄₀₅ are averaged from at least three experiments and indicated as bars with S.D. (line). In each assay (+), 0.2–0.6 μg of His-eIF5₂₄₁₋₄₀₅ was bound to GST-eIF2β₁₋₁₄₀. p values for the increase due to bridging by His-eIF5₂₄₁₋₄₀₅ are shown below. C, co-immunoprecipitation. Cell extracts were prepared from KAY6 (TIF34, C) or KAY107 (HA-TIF34, HA) transformants carrying an empty vector YCplac111 (Vec), YCpL-SUI1-M1 (M1), or YCpL-SUI1-M2 (M2) (Table 1) and subjected to anti-HA immunoprecipitation as described (9). The entire immunoprecipitates (lanes under P) were analyzed by immunoblotting with antibodies specific to factors indicated to the left, together with 20% input (I) and 10% supernatant (S) fractions.

yeast carrying chromosomal *sui1* deletion and a centromeric *URA3* eIF1 plasmid. All of the sc eIF1-NTT mutant plasmids (M1, M2, and M3) replaced the *URA3* eIF1 plasmid in the *sui1Δ* background, indicating that the NTT mutations are not lethal (data not shown). Interestingly, the resulting M1 and M3 strains carrying the mutant protein as the sole eIF1 source grew slowly in the complex-rich medium at the permissive temperature of 30 °C and more slowly at a higher temperature (Fig. 5A, rows 2 and 4). Yeast mutant with *SUI1-Δ20* that was deleted in the NTT region from residues 2–21 was also viable, since the mutant strain grew just like wild-type (Fig. 5A, row 6). These results suggest that the NTT mutations M1 and M3 negatively affect yeast growth and translation. Immunoblot analysis shows that all of the employed eIF1 mutants were expressed at a level nearly identical to or higher than that of the wild-type eIF1 (Fig. 5B). Thus, the eIF1-NTT is not essential for yeast growth, and

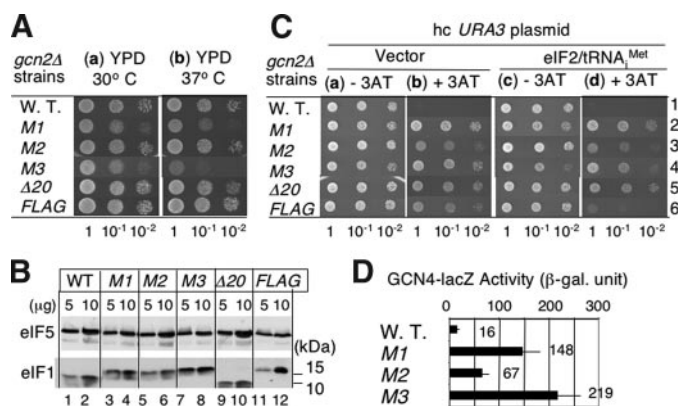


FIGURE 5. Effect of eIF1-NTT mutations on growth and general control phenotypes. A, *Slg*⁻ (slow growth); C, *Gcd*⁻ phenotypes of the site-directed mutants. KAY230 (*Δgcn2*) and its eIF1 mutant derivatives (Table 1, column 6) were spotted on YPD (A) and SD + Ura (C) plates with (+) or without (-) 30 mM 3-aminotriazole and incubated at the indicated temperatures for 2 days (A) or at 30 °C (C) for 3 days (a and c) or 5 days (b and d), respectively. Spots are 10-fold dilutions starting at *A*₆₀₀ = 0.015. FLAG, the *FL-SUI1** allele encoding FL-eIF1. B, the indicated amounts of whole cell extract prepared from all of the *Δgcn2* strains used in A and C were analyzed by SDS-PAGE followed by immunoblotting with rabbit polyclonal antibodies against eIF5 and eIF1. D, transformants of *Δgcn2* strains used in A and C (rows 1–4) carrying the wild-type *GCN4-lacZ* fusion plasmid p180 were grown in SC-ura medium and assayed for β-galactosidase, as described (14). Presented are average values (bars) and S.D. values (bars) from more than six experiments.

hence, its role in MFC assembly is only stimulatory (see "Discussion").

In contrast, M4 and M5, altering the basic binding faces, were unconditionally lethal when examined by plasmid shuffling with the corresponding YCpL-SUI1 derivatives (data not shown) or with the high copy (hc) YEpL-SUI1 derivatives (Fig. 6A). Since the mutant protein was overexpressed from the hc plasmids beyond the level of endogenous eIF1 (Fig. 6B), the lethality of the mutants is due to their functional defect. Thus, both of the basic interfaces of eIF1 mediate essential functions in translation initiation.

Evidence That eIF1-NTT Promotes TC Binding to the Ribosome in Vivo—To further study eIF1-NTT *in vivo*, we used the *GCN4*-dependent general (amino acid) control response as a sensitive indicator of eIF activities (2). *Gcn4p* encodes a transcription factor that activates transcription of genes controlled under the general amino acid control response. Translation of *GCN4* mRNA is regulated by a mechanism involving a series of four short upstream ORFs (uORFs) in its 5' leader. Under non-starvation conditions, translation reinitiation between uORF1 and one of the uORFs from uORF2 to -4 occurs rapidly, dissociating ribosomes from *GCN4* mRNA and repressing *GCN4* translation. However, upon amino acid starvation, the *Gcn2p* eIF2α kinase is activated to lower the eIF2-GTP-Met-tRNA^{Met} TC level. This slows ribosomes' acquisition of TC following uORF1 translation, allowing them to bypass inhibitory uORFs. Thus, *GCN4* is induced (derepressed) during amino acid starvation, conferring a 3-aminotriazole-resistant growth. When eIF mutations decrease the cellular TC level or TC binding to the ribosome, the ribosomes migrating along *GCN4* mRNA after uORF1 translation bypass uORF2 to -4, hence inducing *GCN4* translation in the absence of amino acid starvation signal; *GCN4* translation is constitutive, occurring even in the

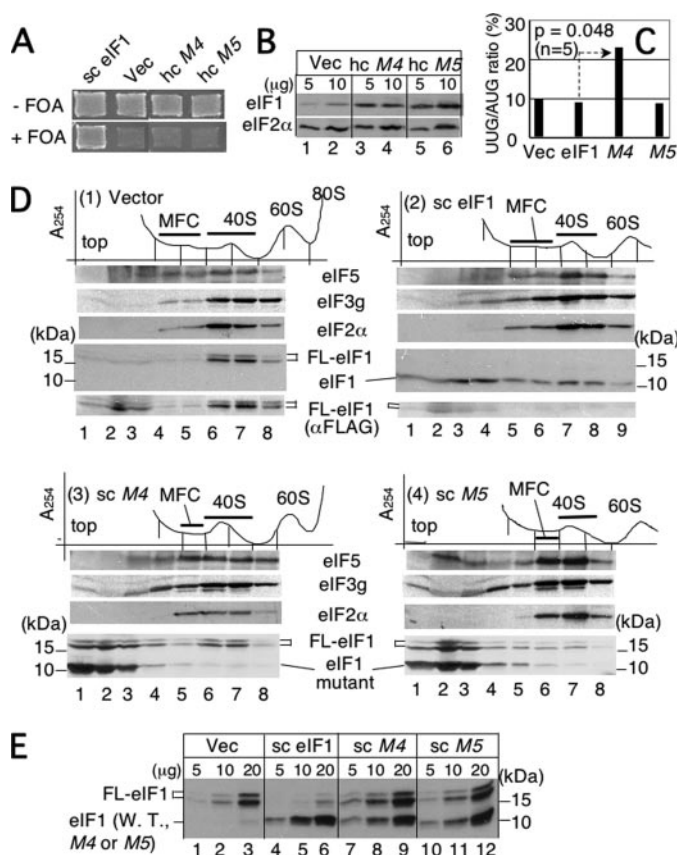


FIGURE 6. The effect of eIF1 mutations altering the basic interfaces in vivo. **A**, the KH and KR areas of eIF1 are essential. Patches of KAY231 ($\Delta gcn2 \Delta sui1$) transformants carrying YCpL-SUI1 (sc eIF1), YEplac181 (Vec.), YEpl-SUI1-M4 (hc M4), or YEpl-SUI1-M5 (hc M5) were replica-plated to SC-Leu plates with (+) or without (–) FOA and incubated for 3 days. FOA sensitivity indicates that the tested allele is lethal. **B**, the indicated amounts of whole cell extract from the same transformants as used in **A**, except one with YCpL-SUI1, grown in SC-Leu medium, were subjected to immunoblotting with rabbit polyclonal anti-eIF2 α or eIF1 antibodies. **C**, Sui[–] phenotype test. Double transformants of F252 (a *ura3-52 leu2-3 his4-303*) carrying a high copy plasmid expressing the eIF1 forms, indicated at the bottom, or an empty vector (Vec), and a *HIS4-lacZ* fusion plasmid with wild-type start codon or one altered to UUG were grown in SC-Ura-Leu medium and assayed for β -galactosidase as in Fig. 5D. The graph shows the average ratio (percentage) of the expression from the UUG reporter over that from the wild-type reporter from five independent experiments. In each experiment, the average values from two independent measurements were used to calculate the UUG/AUG ratio. The S.D. value for the measurement was within 30% of the obtained values. Plasmids used are the same as in **A**, except the hc eIF1 plasmid YEpl-SUI1 (hc eIF1). **D**, effect on eIF1 recruitment to the ribosome in vivo. WCE from transformants of KAY178 (FL-SUI1*) carrying YCplac33 (Vec), YCpU-SUI1 (sc eIF1), or its indicated mutant derivatives (Table 1) were subjected to sucrose gradient analysis after ribosomal complexes were treated with cycloheximide and formaldehyde but not with heparin. Top, A_{254} profile with position of ribosomal species. Bottom gels, gradient fractions were analyzed by immunoblotting with antibodies against the indicated protein; top gel, anti-yeast eIF5; second gel, anti-yeast eIF3g; third gel, anti-yeast eIF2 α ; fourth gel, anti-yeast eIF1; fifth gel (panels 1 and 2 only), anti-FLAG (mouse monoclonal; Sigma). **E**, the indicated amounts of WCE in **D** were analyzed by SDS-PAGE followed by immunoblotting with rabbit polyclonal anti-eIF1 antibodies.

absence of the activator Gcn2p (general control derepressed, or Gcd[–], phenotype).

Yeast *gcn2* Δ strains are sensitive to 3-aminotriazole due to an inability to express the general control response (Fig. 5C, row 1). All of the *gcn2* Δ strains carrying the eIF1-NTT mutations were clearly 3-aminotriazole-resistant (Fig. 5C), with an attendant increase in *GCN4-lacZ* expression from p180 (Fig. 5D), as examined for M1–M3. We previously showed that the FLAG-

eIF1-encoding yeast strain also shows an elevated *GCN4* expression (9). Thus, these mutations derepress the Gcn4p-dependent general control even in the absence of Gcn2p (Gcd[–]). hc TC suppressed the Gcd[–] phenotype of the FLAG-eIF1 construct, indicating that this phenotype results from a defect in TC recruitment to the 40 S subunit (Fig. 5C, row 6), like Gcd[–] phenotypes of eIF3c and eIF5-CTD mutants (7, 28) or the eIF1 9–12 mutant also altering the NTT (17). These results support our previous proposal that eIF1-NTT is involved in TC binding to the ribosome through contributing to MFC formation.

Interestingly, however, hc TC had little or no effect on Gcd[–] phenotypes of other eIF1-NTT mutants (Fig. 5C, d), suggesting that these latter phenotypes are not due to a tRNA^{Met} recruitment defect. The observation made with M1 and M3 may be complicated by their rather toxic effect on yeast growth in the rich medium (Fig. 5A). However, the lack of Gcd[–] phenotype suppression for M2 and $\Delta 20$ mutations, which did not produce any growth defect, contrasts with the Gcd[–] phenotypes by N-terminal FLAG tagging (this study) and 9–12 mutation (17). Thus, Gcd[–] phenotypes of eIF1-NTT mutants appear to be confounded by the effect on processes in initiation other than TC binding to the ribosome (see “Discussion”).

The KH Area Mediates the Essential Function of eIF1 in AUG Selection—The eIF mutations increasing the eIF2 GTPase activation (29) or spontaneous eIF1 release (4) relax stringency of start codon selection and allow translation from UUG codons (Sui[–], or suppressor of initiation codon mutation phenotype). We tested the Sui[–] phenotypes of our eIF1 mutants by reporter assays using *HIS4-lacZ* alleles with altered start codons. The efficiency of translation of the mutant *his4-lacZ* allele from the UUG codon is between 2 and 10% of that of wild-type *HIS4-lacZ* from normal AUG codon in wild-type yeast, depending on the strain background. Sui[–] mutations would significantly increase this ratio. We found that none of the viable NTT mutations tested, M1, M2, or M3, showed the Sui[–] phenotype (data not shown). However, the lethal M4 mutation altering the KH area, but not the M5 mutation altering the KR area, significantly increased translation from UUG codons in a dominant fashion when the mutant protein was expressed from a hc plasmid (Fig. 6C). This suggests that the KH area of eIF1 is important for stringent AUG selection by the ribosome.

To test if the lethal mutant eIF1 proteins are firmly anchored to MFC or the preinitiation complex, we expressed them from sc plasmids in a strain encoding FLAG-eIF1 (used in Fig. 5). The purpose of expression in this strain is to differentiate the plasmid-borne eIF1 mutant from the host-encoded FLAG-eIF1 by size (9). As shown in Fig. 6D, panel 1, sucrose gradient analyses indicated that, in the absence of other eIF1 species, FLAG-eIF1 bound to the 40 S subunit (lanes 6 and 7) without firmly associating with the free MFC (lanes 4 and 5), in agreement with the defect of FLAG-eIF1 observed *in vitro* (9) and *in vivo* (Fig. 5C, row 6). When wild-type eIF1 was expressed, the majority of eIF1 species associated with the 40 S subunit was the wild-type eIF1 (lanes 7 and 8) due to lower abundance of FL-eIF1 in the presence of wild-type eIF1 (Fig. 6E, lanes 1–6). Immunoblotting with anti-FLAG (Fig. 6D, panel 2, bottom gel) indicated that a much smaller fraction of FL-eIF1 bound to the 40 S subunit in lanes 7 and 8 than in the absence of wild-type eIF1 (panel 1,

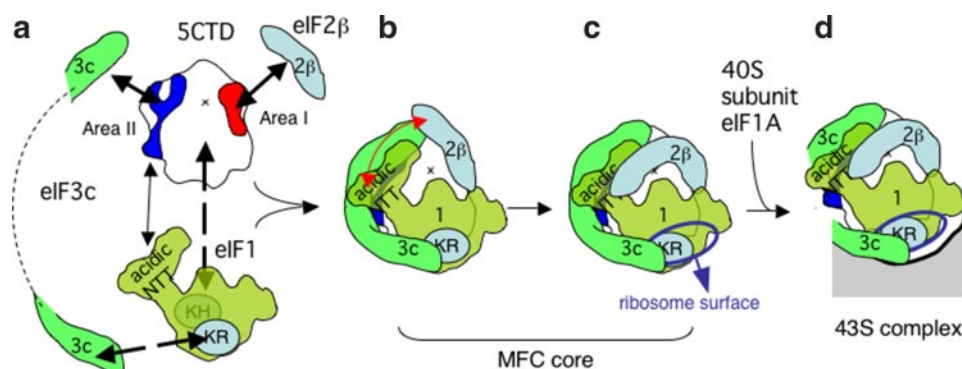


FIGURE 7. Model of MFC assembly with eIF5-CTD as an essential assembly core. eIF1 and eIF5-CTD are depicted with the outline of a space-filled model, together with the partners in each step of preinitiation complex assembly. On eIF1, blue circles represent the basic surfaces; the area KR or KH is located on the side toward or away from the viewer, respectively. In all of the panels (a–d), eIF5-CTD is outlined in the same orientation as in a, with E396 (indicated by x) at the start of the C-terminal tail (aa 396–405) closest to the viewer. Acidic area I and basic area II of eIF5-CTD are drawn in red and blue, respectively. The 40S ribosome surface near the P-site is depicted in gray. NTTs of eIF2β (light blue) and eIF3c (light green) are depicted as hypothetical tubes that wrap around the eIF1/eIF5-CTD core complex. In a, thick arrows indicate essential interactions mediating the MFC. Dashed thick arrows also indicate essential interactions, but they are likely to be essential at later steps in the preinitiation complex function. The interacting surface of eIF5-CTD for eIF1-KH is approximate.

bottom two gels, lanes 6 and 7). These results suggest that the ectopically expressed wild-type eIF1 outcompeted the host-encoded FLAG-eIF1 from the 40S subunit. (As shown in Fig. 6E, lanes 1–6, however, the cellular abundance of FLAG-eIF1 was severely reduced in the presence of wild-type eIF1 for an unknown reason. Thus, we could not rule out the possibility that the reduced binding of FL-eIF1 to the 40S subunit was due to its reduced abundance.)

Importantly, sc eIF1-M4 and eIF1-M5 did not bind to the 40S subunit (Fig. 6D, panels 3 and 4), demonstrating a defect in the 40S subunit binding. Compared with the vector control (panel 1), smaller fractions of FL-eIF1 bound to the 40S subunit in the presence of these eIF1 mutants (panel 3, lanes 6 and 7, and panel 4, lane 7), suggesting that eIF1-M4 and eIF1-M5 can inhibit FL-eIF1 binding to the 40S subunit, possibly by competing with FL-eIF1 for MFC partners albeit weakly (see below). Furthermore, less eIF1-M4 or eIF1-M5 was found in the MFC peak (panels 3 and 4), consistent with their defective binding to MFC partners (Figs. 2 and 3). These results together confirm that the KR area altered by M5 is both a part of the 40S subunit binding face (16) and an MFC incorporation site via eIF3c (Fig. 2) and further indicate that the KH area altered by M4 is an indirect but critical 48S complex binding site. Together with a strong *Sui*[−] phenotype with the eIF1 93–97 mutant altering Ile⁹³, Leu⁹⁶, and Gly⁹⁷, found in the KH area (also see Fig. 2A) and the demonstration of its spontaneous release from a simplified 48S complex *in vitro* (17), our results suggest that the direct interaction of eIF5-CTD with eIF1-KH mediates the critical link of eIF1 to the 48S complex that prevents its release before start codon selection.

DISCUSSION

The structure of yeast eIF1 presented here was used as a basis for identifying binding faces for MFC components. The NMR titration experiments identified two well defined eIF1 regions important for eIF5-(241–405) binding, although the spectro-

scopic changes were small, in part due to the experimental conditions of high salt we had to use. The interaction between these proteins is known to be salt-dependent (9), with higher salt concentrations resulting in weaker binding. All NMR binding experiments had to be conducted at 1 M NaCl due to inherent aggregation of eIF5-(241–405) at low salt (data not shown), thus sacrificing the strength of the interaction to maintain readability of the spectra. Despite being weak, the interactions identified are very specific even at high salt concentration; lowering the salt concentration gradually increases the affinity but is not expected to change the geometry of the complex.

Besides the experimental conditions, the apparently weak effect of eIF5-(241–405) on ¹⁵N-labeled eIF1-His (Fig. 1) may also be due to the C-terminal His tag introduced, which would perturb interaction at the KH area made of eIF1 C-terminal residues. Consistent with this, the eIF1-His allele is lethal when expressed from an sc plasmid, as observed with the eIF1-FL allele (9). In contrast, the N-terminal His tagging shows no growth or Gcd phenotype (see supplemental materials), confirming that although His-eIF1 may be partially defective in eIF5 binding, this is not sufficient to severely impact MFC assembly due to the mutual cooperativity of the complex formation. Understanding why the sc eIF1-His or eIF1-FL allele is lethal would require better understanding of the preinitiation complex components that bind the KH area during the postassembly steps, as discussed below.

Of the two eIF5 interfaces, we provided substantial evidence that eIF1-NTT plays a stimulatory role in MFC assembly both *in vitro* (Figs. 3 and 4A) and *in vivo* (Fig. 4C). That this function of eIF1-NTT is not essential (Fig. 5A) is consistent with the previous finding that human eIF1 deleting the NTT can promote formation of the reconstituted 48S complex on the start codon *in vitro* (16). Together with the recent findings of Cheung *et al.* using the eIF1 9–12 mutant (17), these results establish that the interaction of eIF1-NTT with eIF5-CTD, as observed in Fig. 1, is an important part of MFC-linking interactions. However, the stimulatory, but not essential, function for eIF1-NTT in MFC assembly should not be taken as evidence against the crucial role played by the MFC formation. We previously showed that eIF5-CTD bridges the interaction between eIF2β and eIF3c (11) and that point mutations in eIF5-CTD produce temperature-sensitive (*Ts*[−]) and Gcd[−] phenotypes that are suppressible by hc TC (28) (thick arrows in Fig. 7a). These results provide strong evidence that the eIF5-CTD plays an essential role in Met-tRNA^{Met} recruitment to the ribosome and hence in 43S complex assembly. We propose that eIF1-NTT assists the eIF5-CTD-driven MFC assembly by providing mutual cooperative

interaction faces, as illustrated in Fig. 7a (*thin arrow*) and Fig. 7b (*red arrow*) (also see below).

Our finding that Gcd[−] phenotypes caused by eIF1-M2 and -Δ20 mutants were not suppressed by hc TC (Fig. 5C) suggests that eIF1-NTT is also involved in other steps of translation initiation. For example, if these mutants delay response to AUG recognition, the ribosomes that have acquired TC before GCN4 uORF start codons may skip these codons, such that they instead translate GCN4. This mechanism can lead to a Gcd[−] phenotype that is not suppressible by hc TC. Since the NTT and CTT of eIF1A are implicated in regulating ribosome conformation during the scanning and AUG selection processes (30), it would be intriguing to investigate the role of eIF1-NTT in these processes.

We also presented evidence that the basic part of the second eIF5 interface termed KH plays an essential role and probably regulates AUG selection (Fig. 6, A–C, and a *dashed thick line* in Fig. 7a). The direct interaction would place eIF5 near the decoding site of the 40 S subunit via eIF1 bound near the P-site. Together with the finding of Cheung *et al.* (17) that the hydrophobic part of this surface is critical for suppressing eIF1 release prior to AUG selection, it is conceivable that eIF5-CTD provides the critical link of eIF1 in the scanning preinitiation complex. In agreement with this, we showed that eIF5-CTD is also important for maintaining the integrity of the scanning preinitiation complex (14). However, Lomakin *et al.* (16) also noted that tRNA_i^{Met} is in proximity to the KH area in the human eIF1-tRNA_i^{Met}-40 S complex. Identification of the partner(s) of eIF1-KH during the postassembly processes is an attractive aim of further studies.

Finally, are the eIF1•eIF5-CTD interactions as observed in Fig. 1 retained throughout the initiation process? As illustrated in Fig. 7a, we believe that this is the case at least at the initial MFC assembly step, since eIF1-M4 altering the KH area appears to reduce the interaction with the eIF2β-(1–140)•eIF5-(241–405) complex (Fig. 4, A and B) as well as its incorporation into MFC *in vivo* (Fig. 6D). Since the second basic surface of eIF1 termed KR binds the eIF3c peptide (Fig. 2), it is possible that the eIF3c peptide wraps around the eIF1•eIF5 complex in MFC by binding to eIF1-KR and the eIF3c-binding basic surface of eIF5-CTD termed area II (14) (Fig. 7, b–d). More work combining genetic, biochemical, and structural approaches is needed to study factor communication during translation initiation.

Acknowledgments—We are indebted to Assen Marintchev for comments on this work and Alan Hinnebusch, Tom Dever, Tom Donahue, and John McCarthy for the generous gift of antibodies.

REFERENCES

1. Pestova, T. V., Lorsch, J. R., and Hellen, C. U. T. (2007) in *Translational Control in Biology and Medicine* (Mathews, M. B., Sonenberg, N., and Hershey, J. W. B., eds) pp. 87–128, Cold Spring Harbor Laboratory Press, Cold Spring Harbor, NY
2. Hinnebusch, A. G., Dever, T. E., and Asano, K. (2007) in *Translational Control in Biology and Medicine* (Mathews, M. B., Sonenberg, N., and Hershey, J. W. B., eds) pp. 225–268, Cold Spring Harbor Laboratory Press, Cold Spring Harbor, NY
3. Algire, M. A., Maag, D., and Lorsch, J. R. (2005) *Mol. Cell* **20**, 1–12
4. Maag, D., Fekete, C. A., Gryczynski, Z., and Lorsch, J. R. (2005) *Mol. Cell* **17**, 265–275
5. Passmore, L. A., Schmeing, T. M., Maag, D., Applefield, D. J., Acker, M. G., Algire, M. A., Lorsch, J. R., and Ramakrishnan, V. (2007) *Mol. Cell* **26**, 41–50
6. Pestova, T. V., and Kolupaeva, V. G. (2002) *Genes Dev.* **16**, 2906–2922
7. Valásek, L., Nielsen, K. H., Zhang, F., Fekete, C. A., and Hinnebusch, A. G. (2004) *Mol. Cell. Biol.* **24**, 9437–9455
8. Asano, K., Clayton, J., Shalev, A., and Hinnebusch, A. G. (2000) *Genes Dev.* **14**, 2534–2546
9. Singh, C. R., Hui, H., Li, M., Yamamoto, Y., and Asano, K. (2004) *J. Biol. Chem.* **279**, 31910–31920
10. Asano, K., Krishnamoorthy, T., Phan, L., Pavitt, G. D., and Hinnebusch, A. G. (1999) *EMBO J.* **18**, 1673–1688
11. Singh, C. R., Yamamoto, Y., and Asano, K. (2004) *J. Biol. Chem.* **279**, 49644–49655
12. Wei, Z., Xue, Y., Xu, H., and Gong, W. (2006) *J. Mol. Biol.* **359**, 1–9
13. Bieniossek, C., Schütz, P., Bumann, M., Limacher, A., Uson, I., and Baumann, U. (2006) *J. Mol. Biol.* **360**, 457–465
14. Yamamoto, Y., Singh, C. R., Marintchev, A., Hall, N. S., Hannig, E. M., Wagner, G., and Asano, K. (2005) *Proc. Natl. Acad. Sci. U. S. A.* **102**, 16164–16169
15. Fletcher, C. M., Pestova, T. V., Hellen, C. U. T., and Wagner, G. (1999) *EMBO J.* **18**, 2631–2639
16. Lomakin, I. B., Kolupaeva, V. G., Marintchev, A., Wagner, G., and Pestova, T. V. (2003) *Genes Dev.* **17**, 2786–2797
17. Cheung, Y.-N., Maag, D., Mitchell, S. F., Fekete, C. A., Algire, M. A., Takacs, J. E., Shirokikh, N., Pestova, T., Lorsch, J. R., and Hinnebusch, A. (2007) *Genes Dev.* **21**, 1217–1230
18. Yoon, H. J., and Donahue, T. F. (1992) *Mol. Cell. Biol.* **12**, 248–260
19. Asano, K., Phan, L., Anderson, J., and Hinnebusch, A. G. (1998) *J. Biol. Chem.* **273**, 18573–18585
20. He, H., von der Haar, T., Singh, R. C., Li, M., Li, B., McCarthy, J. E. G., Hinnebusch, A. G., and Asano, K. (2003) *Mol. Cell. Biol.* **23**, 5441–5445
21. Gietz, R. D., and Sugino, A. (1988) *Gene (Amst.)* **74**, 527–534
22. Zhou, P., Lugovskoy, A. A., and Wagner, G. (2001) *J. Biomol. NMR* **20**, 11–14
23. Qiu, H., Garcia-Barrio, M. T., and Hinnebusch, A. G. (1998) *Mol. Cell. Biol.* **18**, 2697–2711
24. Boeke, J. D., LaCroute, F., and Fink, G. R. (1984) *Mol. Gen. Genet.* **197**, 345–346
25. Marintchev, A., Kolupaeva, V. G., Pestova, T. V., and Wagner, G. (2003) *Proc. Natl. Acad. Sci. U. S. A.* **100**, 1535–1540
26. Asano, K., Shalev, A., Phan, L., Nielsen, K., Clayton, J., Valasek, L., Donahue, T. F., and Hinnebusch, A. G. (2001) *EMBO J.* **20**, 2326–2337
27. Nielsen, K. H., Szamecz, B., Valasek, L., Jivotovskaya, A., Shin, B. S., and Hinnebusch, A. G. (2004) *EMBO J.* **23**, 1166–1177
28. Singh, C. R., Curtis, C., Yamamoto, Y., Hall, N. S., Kruse, D. S., Hannig, E. M., and Asano, K. (2005) *Mol. Cell. Biol.* **25**, 5480–5491
29. Huang, H., Yoon, H., Hannig, E. M., and Donahue, T. F. (1997) *Genes Dev.* **11**, 2396–2413
30. Fekete, C. A., Mitchell, S. F., Cherkasova, V. A., Applefield, D., Algire, M. A., Maag, D. K. S. A., Lorsch, J. R., and Hinnebusch, A. (2007) *EMBO J.* **26**, 1602–1614

**Eukaryotic Initiation Factor (eIF) 1 Carries Two Distinct eIF5-binding Faces
Important for Multifactor Assembly and AUG Selection**

Mikhail Reibarkh, Yasufumi Yamamoto, Chingakham Ranjit Singh, Federico del Rio,
Amr Fahmy, Bumjun Lee, Rafael E. Luna, Miki Ii, Gerhard Wagner and Katsura Asano

J. Biol. Chem. 2008, 283:1094-1103.

doi: 10.1074/jbc.M708155200 originally published online November 1, 2007

Access the most updated version of this article at doi: [10.1074/jbc.M708155200](https://doi.org/10.1074/jbc.M708155200)

Alerts:

- [When this article is cited](#)
- [When a correction for this article is posted](#)

[Click here](#) to choose from all of JBC's e-mail alerts

Supplemental material:

<http://www.jbc.org/content/suppl/2007/11/02/M708155200.DC1>

This article cites 29 references, 19 of which can be accessed free at
<http://www.jbc.org/content/283/2/1094.full.html#ref-list-1>